

# A Rotating Platform for Swift Acquisition of Dense 3D Point Clouds

Tobias Neumann, Enno Dülberg, Stefan Schiffer and Alexander Ferrein

Mobile Autonomous Systems & Cognitive Robotics (MASCOR) Institute  
FH Aachen University of Applied Sciences, Aachen, Germany  
{t.neumann, s.schiffer, ferrein}@fh-aachen.de,  
enno.duelberg@alumni.fh-aachen.de

**Abstract** For mapping with mobile robots the fast acquisition of dense point clouds is important. Different sensor techniques and devices exist for different applications. In this paper, we present a novel platform for rotating 3D and 2D LiDAR sensors. It allows for swiftly capturing 3D scans that are densely populated and that almost cover a full sphere. While the platform design is generic and many common LRF can be mounted on it, in our setup we use a Velodyne VLP-16 PUCK LiDAR as well as a Hokuyo UTM-30LX-EW LRF to acquire distance measurements. We describe the hardware design as well as the control software. We further compare our system with other existing commercial and non-commercial designs, especially with the FARO Focus<sup>3D</sup> X 130.

## 1 Introduction

In a number of domains *Mobile Mapping* is used for acquiring range data of the environment. The applications range from light detection and ranging (LiDAR) imaging to find out, say, if heavy-load trucks fit through a height-restricted area to services like Google Street View and other GIS for reconstructing exact street maps or complete urban areas by imaging from cars or aircrafts, respectively. Mobile Mapping in the field of robotics has further important applications. Mobile robot systems may use the acquired information for localisation, but they might also use the incoming sensor information for collision avoidance, terrain classification or path-planning. Outside, a GPS signal can be used for integrating a series of single sensor data into a consistent model of the environment; however, in indoor environments such information is not available. Here, good positioning information of the robot between consecutively recorded sensor readings is required. This information can be computed from overlapping sensor data, for instance, with Structure from Motion approaches in the case of 2D camera images, e.g. [4], or with the Iterative Closest Point (ICP) algorithm for 3D range data, e.g [1,12]. For these methods to work, there must be sufficient overlap between consecutive images or scans. Pomerlau et al. [12] give a number of use cases for ICP-based point cloud registration, ranging from urban search & rescue data acquisition to autonomous driving applications.

For mobile robotic mapping applications, one can distinguish several different modes of how map data is acquired:

1. mapping of static vs. dynamic environments, i.e. whether there are dynamic objects in the environment such as pedestrians;
2. mobile vs. static data acquisition, i.e. the robot acquires data while standing still or while it is moving, respectively.

There is usually a trade-off between acquiring 3D data at a high frequency, on the one hand, and the accuracy of the data, on the other. Normally, slower devices yield higher accuracies in the scan data. There are several scenarios to be taken into account. In environments where many dynamic obstacles are around, one would usually prefer a high scan frequency, while in static environments long scanning times for a single 3D scan are not problematic. Acquiring 3D data in a dynamic environment with a device that takes about half a minute or more may lead to point clouds that are prone to motion blur and occlusions due to dynamic objects. Scanning the scene with a fast device may not yield the same accuracy and density for a single scan, but acquiring multiple scans (from the same position or from different view points) might allow the detection of dynamic obstacles in the data. Hence, the risk of integrating them into the final model is lower. A famous method for this is shown in [5], where rasterization of the data and using the probability on rasterized cells is used. More methods are described in the literature. A different scenario is the acquisition with a moving device, for instance, if a scanning device is mounted onto a robot or a car. Then again, high frequencies per single 3D scan are advantageous.

In this paper, we present SWAP, a novel sensor platform equipped with a Velodyne VLP-16 PUCK<sup>1</sup> 3D LiDAR and a Hokuyo UTM-30LX-EW<sup>2</sup> 2D laser range finder (LRF). With our rotating platform we are aiming at getting the best from two worlds: it provides point clouds of the whole environment at reasonably high speeds with a high data rate. This is partly due to using a 3D instead of (only) a 2D sensor. In the next section, we give the technical description of our novel sensor platform’s hardware and its control software. In Section 3, we compare our system with several other 3D scanning devices used for mobile mapping applications along with a set of system properties. Further, we compare point clouds taken with our platform with the commercial scanner FARO Focus<sup>3D</sup> X130<sup>3</sup> in Section 4, before we conclude.

## 2 The SWAP Platform

In our own earlier work, we developed a tilting LiDAR device based on the Velodyne HDL-64<sup>4</sup> for acquiring dense 3D point clouds in mobile mapping applications [7]. While the device is very suitable for acquiring 3D dense point clouds (in [6] we used this device for mapping large-scale motorway tunnels), it has some drawbacks when it comes to the distribution of the range measurement in the point cloud. With a tilting scanner, the point clouds are particularly dense

---

<sup>1</sup> <http://velodynelidar.com/vlp-16.html>

<sup>2</sup> [http://www.hokuyo-aut.jp/02sensor/07scanner/utm\\_30lx\\_ew.html](http://www.hokuyo-aut.jp/02sensor/07scanner/utm_30lx_ew.html)

<sup>3</sup> <http://www.faro.com/products/3d-surveying/laser-scanner-faro-focus-3d/overview>

<sup>4</sup> <http://velodynelidar.com/hdl-64e.html>

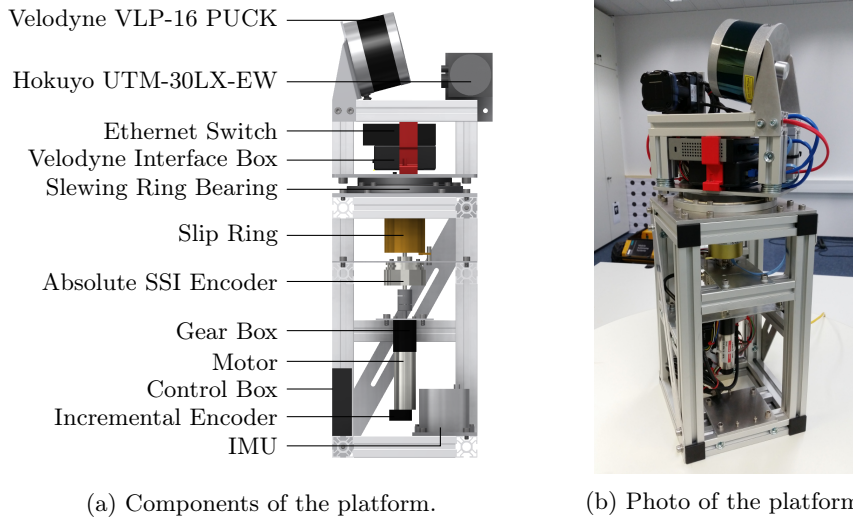


Figure 1: The components and a photo of our rotating sensor platform.

at the turning points of the device. A more even distribution of data is, in general, preferred. For this reason, we developed the SWAP (swift acquisition of point clouds) platform, a rotating 3D LiDAR based on the Velodyne VLP-16 PUCK LiDAR. With the novel system, we achieve a more even distribution of scan points in the point cloud while reducing the time needed for a whole 3D scan. This comes, however, at the cost of the density of the clouds. In the following, we give the technical description of the SWAP platform and its control software.

To be able to acquire the (nearly) complete sphere around the scanning device, we deploy a Velodyne VLP-16 PUCK LiDAR which is rotated perpendicular to its ranging plane. The LiDAR has a vertical field of view (VFoV) of  $30^\circ$  and a horizontal field of view (HFoV) of  $360^\circ$ . The VFoV is scanned with 16 individual laser beams; rotating the LiDAR horizontally yields the range data of the point cloud scanning a complete sphere around the device. The Velodyne is mounted with an inclination of  $14^\circ$  to the vertical rotation axis to maximise the area of high measurement density at the polar region above the platform. By deciding to use this 3D LiDAR we notably increase the number of points that we can register for a scan in a given time while maintaining an equal point distribution. E.g., a 2D LRF would need a frequency of about 300 Hz and capture 900 points in one revolution to acquire a point cloud with a similar resolution within the same time. As the minimum range of the Velodyne starts at about 0.9 m, we additionally mounted a Hokuyo UTM-30LX-EW on our scanning device for close-range data. The UTM-30-LX is a 2D multi-echo LRF with an angular resolution of  $0.25^\circ$ . Its range plane is mounted (almost) perpendicular to the rotating plane of our scanning platform. As a final ingredient, our SWAP platform is equipped with an

inertial measurement unit (IMU) ( $\mu$ IMU from NG<sup>5</sup>) for providing the orientation of the platform w.r.t. the ground. Fig. 1 shows a CAD drawing as well as a photo of the device.

The platform is separated into a base frame and the rotating sensor mount. Both parts are connected with a slip ring and a bearing. The base frame made of industrial aluminium profiles provides low weight and high stiffness which is needed to ensure that the transformation information between the IMU mounted in the lower part and the sensors in the upper part is consistent. The combination of motor and gear head provides us with 3 N m of torque and allows for a maximum rotation speed of 2.6 Hz. However, a reasonable azimuth resolution can only be acquired with a scanning speed of up to 1.67 Hz while the full sphere point clouds are then captured with a half revolution which equals 3.34 Hz for this. Accurate information about the orientation of the rotating sensor platform is essential for correctly registering the raw data of the sensors. We deploy a 14 Bit industrial grade absolute Synchronous Serial Interface (SSI) encoder which is mounted on the drive shaft. The resolution provides a maximum error of 1.32' or 0.022°. In a distance of 10 m, this corresponds to 3.8 mm. The second part of the platform is the rotating sensor mount. It houses a gigabit Ethernet switch, the interface box of the Velodyne VLP-16 PUCK and the Hokuyo UTM-30LX-EW, the power distribution for the sensors and several mounting rails for different sensors.

The raw data of the deployed Velodyne VLP-16 PUCK and the attached Hokuyo UTM-30LX-EW are registered making use of the SSI absolute encoder. Besides the absolute encoders, there is another incremental encoder attached to the motor shaft. Then, based on the readings of the absolute encoder, the raw data is collected and integrated into a point cloud for the device. This is done with a best-effort time-stamping on the data and where one UDP-package of the Velodyne VLP-16 PUCK is transformed all together. The time difference between the laser readings within one UDP-package are about 1.33 ms. For the rectification of the Hokuyo UTM-30LX-EW measurements the recording time for one sweep is taken into account. This setup yields a quite equal distribution of points in the sphere.

### 3 Comparing existing 3D LiDAR Platforms

In the following, we compare our system with a number of other 3D LiDAR devices described in the literature. First, we review some of the devices deployed for 3D mobile mapping. Then, we define system properties of interest in order to compare different scanning devices such as resolution, range or scanning time, before we compare six different 3D scanning devices with our novel platform.

#### 3.1 Acquiring Point Clouds

There are several ways for acquiring 3D point clouds with a mobile robot. One of the most straight-forward ways is to use two 2D LRF which are mounted

<sup>5</sup> <http://www.northropgrumman.litef.com/en/products-services/industrial-applications/product-overview/mems-imu/>

orthogonally to each other. While one sensor is scanning along the XY-plane, the second LRF is mounted in the YZ-plane and measures wall and ceiling distances. However, this way only planar 3D maps [9] can be constructed. Similar setups are described in [3,19]. This sensor setup is suited only for dynamic acquisition, as due to the robot movement different scan lines along the YZ-plane are acquired. This also results in the sensor being unsuitable for collision avoidance.

Another common approach is to tilt one LRF to increase the field of view (FoV) of the ranging device shown, for instance, in [15,14,2]. Tilting, however, has several implications on the point distribution of the point cloud. A more even distribution is achieved by rotating a range device rather than tilting it. The differences between tilting, rolling and yawing an LRF are analysed in [18,10], also w.r.t. the different point densities of the resulting point clouds. Some examples, which we investigate in this section, are the RTS/ScanDrive [18] and its improved version, the RTS/ScanDrive Duo [17] as well as a rotating Hokuyo UTM-30LX-EW range finder described in [13] (which we will call Rotating UTM-30LX or R-UTM-30LX, for short).

The method of an upwards facing LRF which rotates around the yaw-axis as described in [18] is also used in commercial architectural scanning devices where both rotations are already integrated in one system. We will have a closer look at the RIEGL VZ-400<sup>6</sup> and the FARO Focus<sup>3D</sup> X 130. The former was, for instance, deployed in mobile robotics applications in [8], the latter in [16,18]. While both sensors have a horizontal FoV of 360°, the RIEGL VZ-400 has a vertical FoV of 100° with a maximum speed of 6 s for one scan; the FARO Focus<sup>3D</sup> X 130 has a vertical FoV of 300°, here only the occlusion of the sensor platform itself limits the FoV. Other commercial systems such as the Velodyne LiDAR sensors follow a different principle. They use several laser-beams (between 16–64) to capture the VFoV and rotate them horizontally by 360°; they reach a scanning rate of up to 20 Hz. Their sensors have an VFoV between 26.8° and 40°. The Velodyne VLP-16 PUCK used for the 3D scanning device presented in this paper has 16 beams with a 2 degree vertical resolution.

### 3.2 Comparison Methodology

**Mapping Use Case Scenarios.** As pointed out in the introduction, there exist four different scenarios with different requirements for the acquisition sensor:

1. *Static environment:* The environment does not change during the acquisition of a scan. In particular, no dynamic objects occlude parts of the environment.
2. *Dynamic environment:* Dynamic obstacles exist and might cause occlusions or motion blur in the range scans.
3. *Static data acquisition:* While the robot acquires a whole 3D scan (sphere around the robot), the robot stands still.
4. *Dynamic acquisition:* The robot moves while acquiring data; this adds another source of noise into the acquired 3D scan.

<sup>6</sup> <http://www.riegl.com/products/terrestrial-scanning/produktdetail/product/scanner/5/>

The different scenarios pose different requirements to the used 3D ranging device. It is, for example, advantageous if the device achieves a higher scan frequency when used in environments with dynamic obstacles. Consider a robot mapping a human-populated area. A ranging device with a low scanning rate will scan a pedestrian walking past the scanner multiple times, causing the point cloud to be blurred at these positions. Also, the same person occludes larger parts of the environment. On the other hand, if time for acquiring the scan is not of the essence, then the scan frequency is not important. A device then should enjoy a high point rate for providing accurate and dense point clouds of the static environment. This is often the case with architectural scanning devices.

**System Properties.** In the following we clarify which properties of the devices used in our overview will be compared. As, for instance, all devices have different azimuth resolutions, while higher resolutions can be reached with a higher scanning time, we use the fastest possible scanning time with an azimuth resolution of up to  $2^\circ$ .

**Range:** The range yields the maximum distance of the main LiDAR device used in the 3D scanner. The vendors of the devices state the maximal range at different reflectivity values in their data sheets. Therefore, this property just gives an indication of the distances up to which the device can be used.

**Azimuth and Elevation Resolution:** The azimuth resolution shows the horizontal resolution of the scanning device. Likewise, the elevation resolution states the vertical resolution.

**Sphere Coverage:** The sphere coverage  $sc$  indicates the theoretical coverage of a sphere given by the FoV of the sensor. We define it as  $sc = \frac{VFoV \times HFoV}{360^\circ \times 360^\circ}$ . What is also interesting for robotic mapping applications is whether the scanner has blind spots within this acquired sphere. As not all technical details of the scanning devices were available, we could not correlate the blind spots with the sphere coverage. Therefore, the blind spot indicates what is to be expected and covered within the text about each sensor.

### 3.3 System Comparison

In this section, we compare the following devices (also shown in Tab. 1) based on the properties described above.

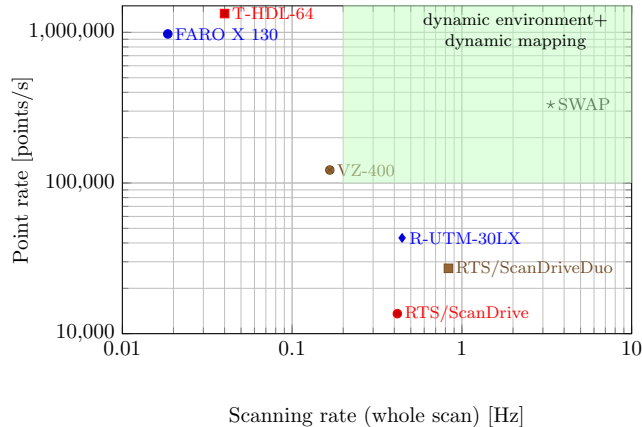
- *RTS/ScanDrive (Duo)*. It is a rotating device with 2 SICK LMS 2D LRFs with a maximal resolution of  $0.25^\circ$ . In [17], the authors describe mapping experiments with this device where they use a resolution of  $1^\circ$ . This is the resolution we refer to in our comparison. The whole device has blind spots at the poles of the scanning sphere, as the two LRFs are mounted with an offset to the rotation centre.

Table 1: Specifications of reviewed systems. The vertical and horizontal resolutions shown correspond to the fastest scanning times of the respective device.

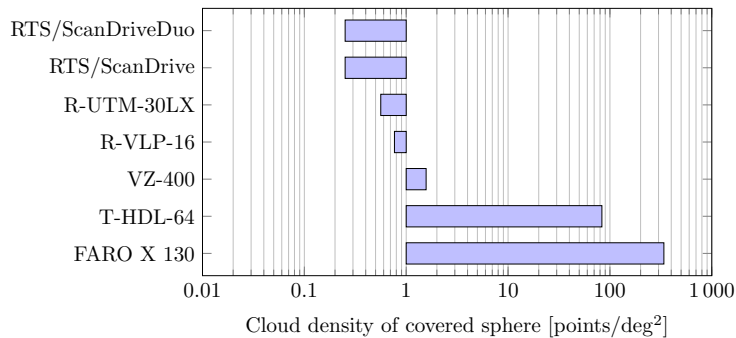
System	Range [m]	Resolution		Sphere coverage
		Horizontal [deg]	Vertical [deg]	[%]
RTS-Duo	30	2	1	100
R-UTM-30LX	30	2	0.25	75
VZ-400	350	0.5	0.288	27.77
Faro X130	130	0.035	0.07	83.33
T-HDL-64	120	0.09	∅0.015	32.44
SWAP	100	2	0.4	80.27

- *R-UTM-30LX*. In [13], mobile mapping applications with a rotating Hokuyo UTM-30LX-EW are described. A single Hokuyo scanner is mounted perpendicular to the rotation plane. Therefore, the vertical resolution in Tab. 1 refers to the physical resolution of the Hokuyo device. The whole device is rotated horizontally. As the scanning time is not given in the paper, we calculated it based on the sensor data sheet for an azimuth resolution of  $2^\circ$ , compared to the RTS/ScanDrive. It covers  $3/4$  of a whole sphere with its scanning range.
- *Riegl VZ-400*. The Riegl VZ-400 is a commercial 3D range scanner. Its vertical resolution lies between  $0.0024^\circ$  and  $0.288^\circ$  and it has a range up to 600 m which, however, can be reduced to 350 m with a reduction in the scanning time. The values given in Tab. 1 show the value when the device is run in its high speed mode. It has a FoV of  $100^\circ \times 360^\circ$ . A complete scan requires 6 s; the device acquires up to 122 000 points/s.
- *FARO X130*. The other commercial scanner in the field is the FARO Focus<sup>3D</sup> X 130. It has a vertical and horizontal resolution of  $0.009^\circ$ , respectively and a maximal range of about 130 m. It has a FoV of  $300^\circ \times 360^\circ$ . A complete scan takes up to 54 s, scanning up to 976 000 points/s.
- *Tilting HDL-64*. As described in [7], a Velodyne HDL-64 LiDAR is tilted between  $0^\circ$  and  $90^\circ$  which results in a VFoV of  $118.6^\circ$  but with a large blind spot which is produced by the robot base where the sensor is mounted on. It has a range of about 120 m. The data rate of the sensor is 1 330 000 points/s. A whole sweep takes about 25 s.

Fig. 2a shows a comparison of the different systems w.r.t. the scanning times and the data rate of the respective 3D scanning devices. Note that both axes have a logarithmic scale. On the  $x$ -axis, the scanning rate in Hz is given. It shows the frequency with which a whole 3D scan (sphere or part of a sphere around the robot) can be acquired. On the  $y$ -axis, the point rate is given. It shows how many points the respective ranging sensor mounted on the device is acquiring per second. Devices such as the FARO or the T-HDL-64 have a high data rate,



(a) A comparison of points/s and scans/s for typical mobile robotics sensors.

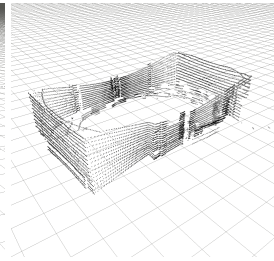
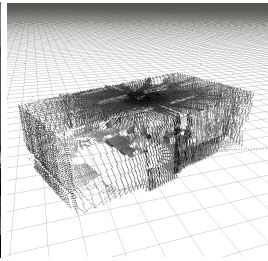
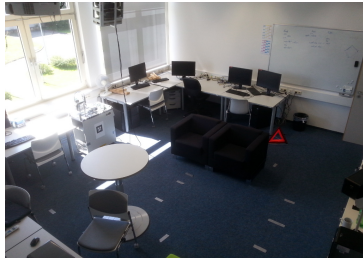


(b) Cloud density

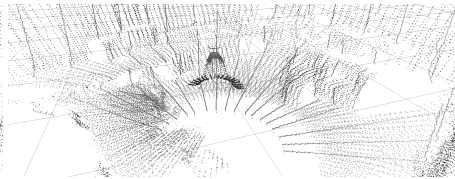
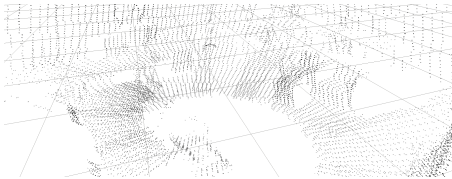
Figure 2: Comparison results.

but a whole sweep takes quite a long time (25 or 54 seconds, respectively). The other rotating devices such as the RTS or the R-UTM-30LX have a reasonable scanning time for a whole 3D sweep, but the data rate is not exceptionally high. Our novel SWAP platform has a really good trade-off between a reasonable scanning rate and a sufficiently high data rate. As shown in Fig. 2a, it is therefore the most suitable for dynamic mapping in dynamic environments.

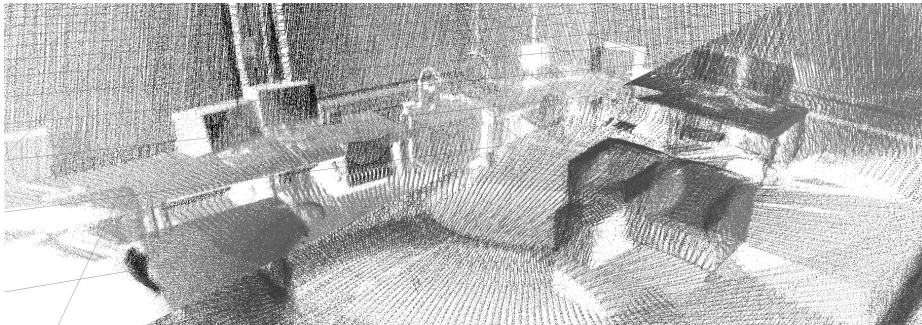
Fig. 2b compares the theoretical point cloud density that can be achieved by the compared devices with the settings given in Tab. 1. We compare the number of points per  $\text{deg}^2$  which the respective device is able to scan. Note that this number is normalised w.r.t. the sphere coverage of the device. The densest point cloud, therefore, is generated by the FARO X 130, which scans over 300 points per  $\text{deg}^2$ . Our novel device produces point clouds which is close to a resolution of  $1 \text{ deg}^2$ , while the platforms with one or two rotating LRFs (RTS + R-UTM-30LX) acquire much sparser point clouds.



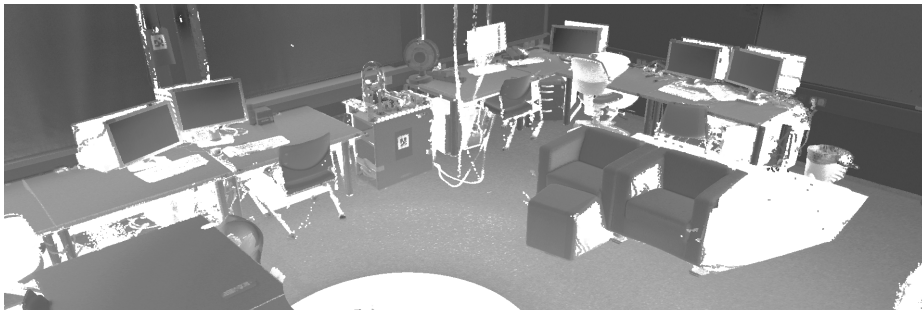
(a) Photo of the captured example (b) Indoor example at 3.34 Hz, full room view (c) VLP-16 without any rotation



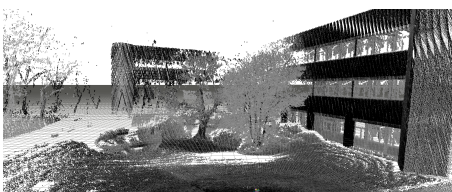
(d) SWAP with point clouds at 3.34 Hz (e) SWAP with point clouds at 1 Hz



(f) Upper left triangle: SWAP with point clouds at 0.033 Hz (30 s) Lower right triangle: The scene captured with five point clouds taken at different positions. The capture time off all clouds together took 50 s.



(g) FARO Focus<sup>3D</sup> X 130 with point clouds at 0.019 Hz (54 s)



(h) Outdoor scene captured by the SWAP platform in 30 s (left) and captured by the FARO Focus<sup>3D</sup> X 130 in 54 s (right) as a comparison.

Figure 3: Example data of the SWAP platform captured with different rotation times and data from the FARO Focus<sup>3D</sup> X 130 as a comparison.

## 4 Discussion

As we have shown in the previous section, there are quite a few 3D scanning devices available. The properties of the scanners are quite different, some target at scanning architecture, some are rather suited for mobile mapping applications. The former devices usually have a high point rate but a very low scanning rate. The FARO Focus<sup>3D</sup> X130 is such a device. The scanners presented in our comparison that fall into the latter class trade a lower point rate for a higher scanning frequency. This makes them more interesting for mobile mapping. As we have shown in the scanner comparison, our rotating platform has a comparably high point rate (w.r.t. the other mobile mapping devices) and a high scanning rate. This makes it especially useful for dynamic mapping applications in dynamic environments.

In the rest of this section, we want to compare scanners not only based on their technical data sheet, but also qualitatively based on the resulting point clouds. In particular, we show point clouds from a scene in our laboratory environment and an outside scene of our university campus, both acquired with a FARO Focus<sup>3D</sup> X130 and the novel SWAP platform.

Fig.3 shows scans from our laboratory. Fig. 3a shows a photograph of the scene to give an overview. Fig. 3b shows a point cloud from the whole laboratory scanned with the SWAP platform in comparison of just deploying the Velodyne VLP-16 PUCK in the same room without rotating it (Fig. 3c). It becomes apparent why the Velodyne sensor needs to be rotated in order to acquire a full scanning sphere. Fig. 3d to 3f show scans of the same scene taken at different rotation speeds of the SWAP device. While at 3.34 Hz the cloud is still somewhat sparse (but dense enough for mapping), the scan at 0.033 Hz is very detailed. The upper triangle of Fig. 3f shows a scan of the lab taken at 0.033 Hz; the cloud in the lower triangle shows an overlay of the whole scene captured from several view points. The total scan times of the different scans sum up to 50 s. This is nearly the time, which the FARO Focus<sup>3D</sup> X130 took from a single view point (Fig. 3g). One has to keep in mind that many point clouds are taken in mobile mapping applications to reconstruct the whole scene. Therefore, even more sparse scans are not a problem. On the contrary, while doing multiple scans taken with a higher frequency, shadows and occlusions that might occur when acquiring data only from one position can be avoided. Finally, we want to show two scans from an outside scene taken at our campus, again from the SWAP platform and the FARO Focus<sup>3D</sup> X130. While the scan from the FARO Focus<sup>3D</sup> X130 again is much more detailed, our rotating platform does not leave out major details of the scene. Note that the scanning time of our scanner compared to the FARO is cut in half. The distance to the campus buildings in the background is about 50 m.

## 5 Conclusion and Future Work

In this paper, we presented a novel platform for acquiring point clouds for robot mapping applications. The main idea is to continuously rotate a 3D LiDAR sensor

around an axis that is perpendicular to its main ranging axis. In our case, we make use of a Velodyne VLP-16 PUCK together with a Hokuyo UTM-30LX-EW. With our setup we achieve more evenly distributed point clouds than with a tilting sensor while reaching nearly a full sphere coverage of the surrounding (only a cone of about  $71^\circ$  towards the sensor base cannot be acquired with the Velodyne VLP-16 PUCK, the occlusion of the Hokuyo UTM-30LX-EW is even lower). We have shown that our system is capable of capturing such full-sphere point clouds at a high speed of up to 3.34 Hz with a density that is still reasonably high enough for collision avoidance and generating 3D maps. This makes the SWAP platform the fastest 3D scanner with a near full-sphere coverage in the set of scanners that have been compared in this paper. Furthermore, we compared the results at slower revolutions with commercially available architecture scanner, yielding satisfyingly dense and accurate point clouds for mobile mapping applications.

The next steps for the system are to change from the best-effort time stamping to a real-time-system. The motor and encoders are currently controlled via USB, but they also support a serial connection, the data of the LiDAR sensors are delivered via Ethernet. The Velodyne VLP-16 PUCK gives a time-table for the time-offset of each laser within a UDP-package and the Hokuyo UTM-30LX-EW has a further synchronous output which sends a 1 ms long signal at a defined position of the laser.

Furthermore, the extrinsic calibration of the sensors needs to be measured precisely for correct range measurements. In [11] an automatic and fast method for this calibration is given which we are planning to adapt for our setup. With this automatic calibration we will measure the accuracy of the system compared to the architecture scanner FARO Focus<sup>3D</sup> X 130 by aligning point clouds of the same area and calculating the mean point error.

**Acknowledgments** This work was funded in part by the German Federal Ministry of Education and Research in the programme under grant 033R126C. We thank the anonymous reviewers for their helpful comments and Christoph Gollok for the simulation of the point distribution in Gazebo.

## References

1. Besl, P.J., McKay, N.D.: Method for registration of 3-D shapes. *IEEE Transactions on Pattern Analysis and Machine Intelligence* 14(2) (Feb 1992)
2. Bohren, J., Rusu, R.B., Jones, E.G., Marder-Eppstein, E., Pantofaru, C., Wise, M., Mösenlechner, L., Meeussen, W., Holzer, S.: Towards autonomous robotic butlers: Lessons learned with the PR2. In: *IEEE International Conference on Robotics and Automation (ICRA)* (May 2011)
3. Früh, C., Zakhor, A.: 3D model generation for cities using aerial photographs and ground level laser scans. In: *Proceedings of the Computer Society Conference on Computer Vision and Pattern Recognition (CVPR)*. vol. 2 (2001)
4. Hartley, R., Zisserman, A.: *Multiple View Geometry in Computer Vision*. Cambridge University Press (2003)

5. Hornung, A., Wurm, K.M., Bennewitz, M., Stachniss, C., Burgard, W.: OctoMap: an efficient probabilistic 3D mapping framework based on octrees. *Autonomous Robots* 34 (2013)
6. Leingartner, M., Maurer, J., Ferrein, A., Steinbauer, G.: Evaluation of sensors and mapping approaches for disasters in tunnels. *Journal of Field Robotics* (2015)
7. Neumann, T., Ferrein, A., Kallweit, S., Scholl, I.: Towards a mobile mapping robot for underground mines. In: *Proceedings of the 7th IEEE Robotics and Mechatronics Conference* (2014)
8. Nüchter, A., Borrmann, D., Koch, P., Kühn, M., May, S.: A Man-Portable IMU-Free Mobile Mapping System. *ISPRS Annals of Photogrammetry, Remote Sensing and Spatial Information Sciences II-3/W5* (2015)
9. Nüchter, A., Lingemann, K., Hertzberg, J., Surmann, H.: 6D SLAM-3D mapping outdoor environments, *Journal of Field Robotics*, vol. 24. Wiley (2007)
10. Nüchter, A.: 3D Robotic Mapping, *Springer Tracts in Advanced Robotics*, vol. 52. Springer (2008)
11. Oberländer, J., Pfozter, L., Roennau, A., Dillmann, R.: Fast calibration of rotating and swivelling 3-d laser scanners exploiting measurement redundancies. In: *Proceedings of the International Conference on Intelligent Robots and Systems (IROS)* (2015)
12. Pomerleau, F., Colas, F., Siegwart, R.: A review of point cloud registration algorithms for mobile robotics. *Foundations and Trends in Robotics* 4(1) (2015)
13. Schadler, M., Stückler, J., Behnke, S.: Multi-resolution surfel mapping and real-time pose tracking using a continuously rotating 2D laser scanner. In: *International Symposium on Safety, Security, and Rescue Robotics (SSRR)* (2013)
14. Surmann, H., Lingemann, K., Nüchter, A., Hertzberg, J.: A 3D laser range finder for autonomous mobile robots. In: *Proceedings of the 32nd International Symposium on Robotics (ISR)* (2001)
15. Thrun, S., Thayer, S., Whittaker, W., Baker, C., Burgard, W., Ferguson, D., Hahnel, D., Montemerlo, D., Morris, A., Omohundro, Z., Reverte, C., W, W.: Autonomous exploration and mapping of abandoned mines. *IEEE Robot. Autom. Mag.* 11(4) (2004)
16. Wong, U., Morris, A., Lea, C., Lee, J., Whittaker, C., Garney, B., Whittaker, R.: Comparative evaluation of range sensing technologies for underground void modeling. In: *Proceedings of the International Conference on Intelligent Robots and Systems (IROS)* (2011)
17. Wulf, O., Nüchter, A., Hertzberg, J., Wagner, B.: Ground truth evaluation of large urban 6D SLAM. In: *Proceedings of the International Conference on Intelligent Robots and Systems (IROS)* (2007)
18. Wulf, O., Wagner, B.: Fast 3D scanning methods for laser measurement systems. In: *Proceedings of the International Conference on Control Systems and Computer Science* (2003)
19. Zhao, H., Shibasaki, R.: Reconstructing textured cad model of urban environment using vehicle-borne laser range scanners and line cameras. In: *Second International Workshop on Computer Vision System (ICVS)* (2001)